

Measuring Tail Risks

Kan Chen^{a,b,*}, Tuoyuan Cheng^a

^a*Risk Management Institute, National University of Singapore, 04-03 Heng Mui Keng Terrace, 13 Building, Singapore, 119613, Singapore*

^b*Department of Mathematics, National University of Singapore, Level 4, Block S17, 10 Lower Kent Ridge Road, Singapore, 119076, Singapore*

Abstract

Value-at-Risk (VaR) and Expected Shortfall (ES) are common high quantile-based risk measures adopted in financial regulations and risk management. In this paper, we propose a tail risk measure based on the most probable maximum size of risk events (MPMR) that can occur over a length of time. MPMR underscores the dependence of the tail risk on the risk management time frame. Unlike VaR and ES, MPMR does not require specifying a confidence level. We derive the risk measure analytically for several well-known distributions. In particular, for the case where the size of the risk event follows a power law or Pareto distribution, we show that MPMR also scales with the number of observations n (or equivalently the length of the time interval) by a power law, $\text{MPMR}(n) \propto n^\eta$, where η is the scaling exponent (SE). The scale invariance allows for reasonable estimations of long-term risks based on the extrapolation of more reliable estimations of short-term risks. The scaling relationship also gives rise to a robust and low-bias estimator of the tail index (TI) ξ of the size distribution, $\xi = 1/\eta$. We demonstrate the use of this risk measure for describing the tail risks in financial markets as well as the risks associated with natural hazards (earthquakes, tsunamis, and excessive rainfall).

Keywords: Risk management, Risk measure, Extreme value, Maximum loss, Power law, Tail index

*Corresponding author: kan.chen@nus.edu.sg

1. Introduction

Measuring tail risk is essential in quantitative risk management. There are a few established measures in financial risk management [1, 2]. Variance or standard deviation of returns is often used as a risk measure in the context of portfolio optimization and risk attribution. It is, however, not a good measure for tail risks as the return distributions of financial assets often exhibit fat tails. Expected Shortfall (ES) and Value-at-Risk (VaR) focus on tail distributions. They are used as key metrics for determining capital requirements in financial regulations and are now widely accepted in portfolio optimization. VaR and ES are specified with a given confidence level in a specific time frame. For example, the market risk is specified using the loss in 10 days with a confidence level of 99% and the credit and operational losses are specified using the loss within one year with a confidence level of 99.9% [3]. VaR is more intuitive and more popular. However, it doesn't satisfy the key sub-additivity condition and is thus not a coherent risk measure [1]. This is the main reason regulators are moving towards adopting ES, which is a coherent measure. In our opinion, the main drawback of VaR and ES is that the confidence level specification is rather subjective. The tail probabilities of losses over different time frames are related; so the confidence level shouldn't be specified independently. Instead, it should be tied to the time frame considered.

The tail part of the size distribution can often be characterized by a power law, which expresses the scaling relationship between the probability of a risk event and its size [4, 5, 6]. There is a vast literature on this subject. In stock markets, the cubic law describing the tail part of the stock return distribution has been established [7, 8, 9, 10]. Kelly and Jiang [11] have further proposed a dynamic tail risk measure, making use of the cross-section of individual stock returns to estimate the common tail index for the conditional tail risk distributions of individual assets. They provide evidence that tail risk has large predictive power for aggregate stock market returns and is important for asset pricing. There is a wide range of instances of frequency-size scaling. The distribution of operational losses can be characterized by a power law [12]. The Gutenberg-Richter law in seismology is perhaps the best-known frequency-size scaling relationship. In hydrology, the scale invariance has also been used to characterize the rainfall intensity-duration-frequency relationship [13, 14]. The frequency-size scaling has been

viewed as a sign of emerging behavior in large interactive complex systems [15, 16, 17]. One possible mechanism, self-organized criticality (SOC), has been proposed to explain the emergence of such scaling relations [18]. The concept of SOC has been applied, for example, to the study of earthquake dynamics [19, 20, 21, 22, 23]. SOC helps to explain the mechanism for the emergence of the Gutenberg-Richter law.

In this paper, we propose a risk measure based on the most probable maximum size of risk events (MPMR) that can occur over a time frame. This measure is generic; it is applicable for describing tail risk in financial systems as well as the risks associated with natural hazards. In the context of financial risks, the size is the financial loss. When defining MPMR for the financial risk we don't consider the total loss over the period as in the case of VaR and ES, but only the maximum of the daily losses (regarding the market risk) or the losses from individual risk events (regarding the operational risk) in the period. We will demonstrate that the dependence of the potential maximum size of risk on the time frame considered reflects the tail size distribution of individual risk events; as the sample size increases, we will likely encounter bigger and rarer events. From the risk management perspective, the maximum loss from a shock (the duration of which is normally much shorter than the risk management time frame) might be more relevant than the total loss of the entire period. It is easy to check that MPMR satisfies the conditions of coherent risk measures. We will explore the use of MPMR and related expected maximum size of risk events (EMR) to characterize financial losses as well as the sizes of risk events due to natural hazards.

2. MPMR, EMR, and their sample size dependence

In this section, we introduce the MPMR and the EMR risk metrics and analyze their sample-size dependence for several underlying distributions.

Let X_1, X_2, \dots, X_n be i.i.d. random variables with density function $f_X(\cdot)$ and distribution function $F_X(\cdot)$ within a sampled block of size n . Let S be the maximum in this block (block maximum) with the density function $f_S(\cdot)$,

we have [24],

$$S = \max_{i=1,2,\dots,n} X_i$$

$$f_S(s) = \frac{\partial(F_X(s))^n}{\partial s} = n f_X(s) (F_X(s))^{n-1} \quad (1)$$

To determine MPMR as the most probable value of S , denoted as s^* , we set $\frac{\partial f_S(s)}{\partial s} \Big|_{s=s^*} = 0$, which gives,

$$\left[\frac{\partial f_X(s)}{\partial s} (F_X(s))^{n-1} + f_X(s)(n-1) (F_X(s))^{n-2} f_X(s) \right] \Big|_{s=s^*} = 0$$

$$\left[\frac{\partial f_X(s)}{\partial s} (F_X(s)) + (n-1)f_X^2(s) \right] \Big|_{s=s^*} = 0 \quad (2)$$

Focusing the leading order of the large sample size limit $n \rightarrow \infty, s \rightarrow \infty, F_X(s) \rightarrow 1$, we have approximately,

$$\left[\frac{\partial f_X(s)}{\partial s} + n f_X^2(s) \right] \Big|_{s=s^*} = 0 \quad (3)$$

equation (2) and equation (3) can be solved numerically via root-finding algorithms when $f_X(\cdot)$ is specified either parametrically or non-parametrically [25].

With others held constant, s^* is a function of n . We now explore the relationship between s^* and n , given several well-known underlying distributions for $f_X(\cdot)$. For the power-law and exponential distributions, we have also obtained the analytical forms of the EMR, which is the expected value of the maximum.

- (i) For the normal distribution, without loss of generality, let $X \sim N(0, \sigma^2)$, $f_X(x) = \frac{1}{\sigma\sqrt{2\pi}} \exp\left(\frac{-x^2}{2\sigma^2}\right)$. From equation (3) we have,

$$s^* \approx \sigma \sqrt{W_0\left(\frac{n^2}{2\pi}\right)}$$

$$\approx \sigma \sqrt{\log\left(\frac{n^2}{2\pi}\right) - \log\left(\log\left(\frac{n^2}{2\pi}\right)\right)}$$

$$\approx \sigma \sqrt{2\log(n)} \left(1 - \frac{\log(\log(n))}{4\log(n)}\right)$$

where $W_0(\cdot)$ is the principal branch of the product logarithm or Lambert W function, which gives the root of $x \exp(x) - y = 0$ [26], and we keep the terms corresponding to the first two leading orders in the large n limit.

- (ii) For the exponential distribution, let $X \sim \text{Exp}(\xi)$, $f_X(x) = \xi \exp(-\xi x)$, and $F_X(x) = 1 - \exp(-\xi x)$. From equation (2) we have,

$$-\xi^2 \exp(-\xi s^*) (1 - \exp(-\xi s^*)) + (n-1) \xi^2 \exp(-2\xi s^*) = 0$$

$$s^* = \frac{\log n}{\xi}$$

$$\mathbb{E}[S] = \int_0^{+\infty} s f_S(s) ds = \frac{\sum_{i=1}^n \frac{1}{i}}{\xi} \approx \frac{\gamma + \log n}{\xi}$$

where $\gamma = \lim_{n \rightarrow \infty} (-\log n + \sum_{i=1}^n \frac{1}{i}) \approx 0.577216$ is the Euler's constant.

- (iii) For the power-law or Pareto type I distribution, let $Y \sim \text{Exp}(\xi)$, we have $X = A \exp(Y) \sim \text{Pareto}(A, \xi)$, $f_X(x) = \frac{\xi A^\xi}{x^{\xi+1}}$, and $F_X(x) = 1 - \frac{A^\xi}{x^\xi}$. From equation (2) we have,

$$-\frac{\xi(\xi+1)A^\xi}{s^{\xi+2}} \left(1 - \frac{A^\xi}{s^\xi}\right) + (n-1) \frac{\xi^2 A^{2\xi}}{s^{2\xi+2}} = 0.$$

The solution ($s = s^*$) of the above equation is given as

$$s^* = A \left(\frac{1 + n\xi}{1 + \xi} \right)^{\frac{1}{\xi}} \approx A \left(\frac{\xi}{1 + \xi} \right)^{1/\xi} n^{1/\xi} \left(1 + \frac{1}{n\xi^2} \right) \quad (4)$$

When $\xi > 1$, using Euler's reflection formula and the reciprocal gamma function [27], we have

$$\mathbb{E}[S] = \int_A^{+\infty} s f_S(s) ds = \frac{A \mathcal{B}(n, 1 - \frac{1}{\xi})}{-\mathcal{B}(-n, 1)} = An \mathcal{B}(n, 1 - \frac{1}{\xi}) \quad (5)$$

$$\approx A \Gamma(1 - \frac{1}{\xi}) n^{\frac{1}{\xi}} + \frac{A \Gamma(2 - \frac{1}{\xi})}{2\xi} n^{\frac{1}{\xi}-1}$$

where $\mathcal{B}(\cdot, \cdot)$ is the beta function and $\Gamma(\cdot)$ is the gamma function.

(iv) The Student's t distribution has a power-law tail. Let $X \sim t(\nu)$, we have:

$$f_X(x) = \frac{\Gamma(\frac{\nu+1}{2})}{\sqrt{\nu\pi}\Gamma(\frac{\nu}{2})} \left(1 + \frac{x^2}{\nu}\right)^{-\frac{\nu+1}{2}}$$

The tail distribution is given by

$$\begin{aligned} f_X(x) &\approx \frac{\nu A^\nu}{x^{(\nu+1)}} \\ s^* &\approx A \left(\frac{1+n\nu}{1+\nu}\right)^{\frac{1}{\nu}} \end{aligned} \tag{6}$$

where $A = \sqrt{\nu} \left(\frac{\Gamma(\frac{\nu+1}{2})}{\sqrt{\pi}\Gamma(\frac{\nu+2}{2})}\right)^{\frac{1}{\nu}}$. When $\nu > 1$, we have:

$$\begin{aligned} \mathbb{E}[S] &\approx An\mathcal{B}(n, 1 - \frac{1}{\nu}) \\ &\approx A \Gamma(1 - \frac{1}{\nu}) n^{\frac{1}{\nu}} + \frac{A \Gamma(2 - \frac{1}{\nu})}{2\nu} n^{\frac{1}{\nu}-1} \end{aligned} \tag{7}$$

For these distributions we consider here, it is easy to check that the leading order dependence of MPMR and EMR (when it exists) on the sample size n , as $n \rightarrow \infty$, is the same. This has been explicitly shown in the cases of the exponential and power-law distributions. Since the tail part of the size distribution of risk events can often be described by the Pareto-type model [5, 6], we will focus on the case of power-law distribution in our tail risk measure study. It can be seen from equations (4) to (7) that MPMR and EMR scale with sample size n with the scaling exponent (SE) $\eta = \frac{1}{\xi}$, or the reciprocal of the tail index (TI), ξ .

3. TI estimator derived from sample-size scaling of MPMR

In this section, we explore the use of sample-size scaling of MPMR to estimate TI for power-law tail distributions and demonstrate that it provides a robust and accurate estimate of TI. Given a sample size of n , we can perform a sub-sampling without replacement from N raw observations to form a block of size n and record its maximum as a block maxima (BM) sample. We obtain the MPMR at this block size n by estimating the mode of M sub-sampled BMs using the mean-shift algorithm [28], whose convergence in

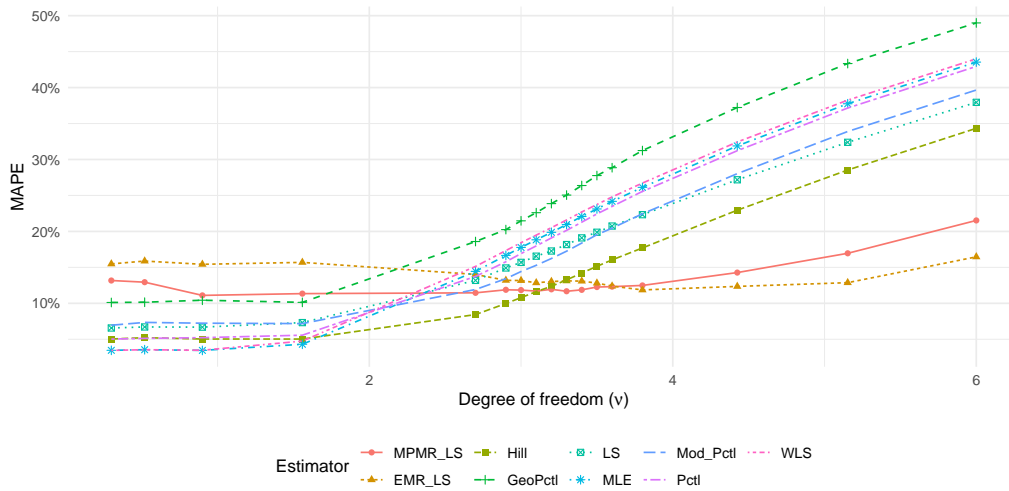
\mathbb{R}^1 is proven [29]. The hyper-parameter bandwidth used in the algorithm is calculated following the rule of thumb in [30]. The EMR at this block size n is simply estimated by taking the sample mean on the M sub-sampled BMs.

With a series of MPMR and EMR at different n , we fit a simple linear regression model to $\log(\text{MPMR}) \sim \log(n)$ and to $\log(\text{EMR}) \sim \log(n)$. We then obtain the estimate of SE $\hat{\eta}$ as the slope of the linear fit. Note that instead of fitting $\log(\text{EMR}) \sim \log(n)$, we can use all the raw BMs to fit a linear regression model to $\log(\text{BM}) \sim \log(n)$ and obtain the same result. The estimated TI $\hat{\xi}$ is given as the reciprocal of $\hat{\eta}$.

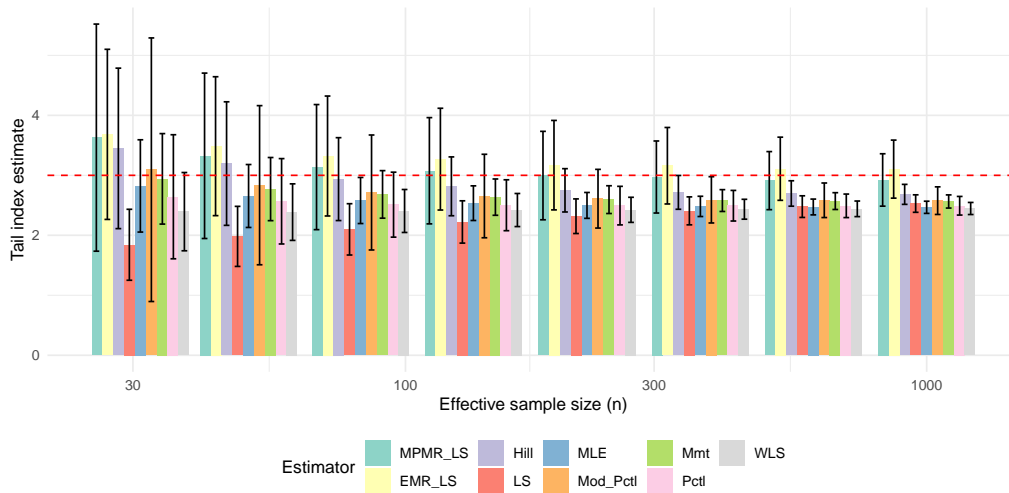
During the sub-sampling step, we set the lower limit for n as $n = 1$, and the upper limit as $n = N(1 - 1/e)$. This is to take up a reasonably wide range of n for regression purposes while avoiding BM estimates at the same n being too concentrated. Considering that we are handling mostly time-series data and the tail distribution is highly non-Gaussian, we selected sub-sampling instead of bootstrapping or upstrapping [31, 32]. Following Ref. [33], we set the number of sub-samples M to 600 at each n .

We conduct simulations to compare our TI estimators based on MPMR to several well-known TI estimators [34, 35], including Hill’s estimator [36], least squares estimator [37], weighted least squares estimator [38], method of percentiles estimator [39], method of modified percentiles estimator [39], maximum likelihood estimator [40], method of geometric percentiles estimator [39], and method of moments estimator [41, 42]. We use Student’s t as the underlying distribution to generate raw samples of various TIs and sample sizes. Only the top 10% of raw samples are picked as effective tail samples of size N for the estimators to work on. From equations (6) and (7), the true TI ξ is equal to the degree of freedom ν . For every combination of effective sample size N and ν , we run 1009 simulations to get the mean, standard deviation and mean absolute percentage error using outcomes from the estimators considered here.

Comparisons are charted in figure 1. Estimators based on MPMR and EMR have good bias-variance trade-offs for various ν as shown in figure 1a. We further fix $\nu = 3$ (to match the cubic law found in stock returns [7]) and show the mean and standard deviation of TI estimates at various effective sample sizes in figure 1b. The MPMR and EMR estimates show consistently



(a) Mean absolute percentage error of TI estimators at various true TIs, with effective sample size = 1000.



(b) Mean and standard deviation of TI estimators at various effective sample sizes, with $\nu = 3$.

Figure 1: Performances of TI estimators, applied on top 10% observations from Student's t distribution.

low biases. Note that for financial markets' daily returns, the tail sample (taking 10% of the top profit and loss values from the raw data sample of around 252 return values in a year) has around 13 effective observations of losses. In such small sample scenarios, MPMR or EMR is a relatively more robust choice. The RBM estimator from Ref. [43] also gives good estimates but requires expensive computation.

4. Stylized facts of MPMR/EMR for describing the natural hazards

In this section, we apply the proposed MPMR and EMR to analyze the tail risks associated with natural hazards. Extreme value analysis is widely accepted to analyze, understand, and predict natural hazard events [4, 44]. The selected examples of natural hazards have significant impacts on human activities, and the associated risks have gradually been quantified and priced in financial markets. There are also ample observation data on these natural hazards over a long history; this makes the statistical analysis of natural hazards a good test for tail risk measures,

4.1. Earthquake

We first consider earthquake statistics. The size-frequency relation of earthquakes is well described by a power law, known as the Gutenberg-Richter law, which states that the probability of an earthquake with a size greater than S is proportional to S^{-b} , or $\mathbb{P}(\text{Size} > S) \propto S^{-b}$. The original GR law is stated as a frequency-magnitude relation, where the magnitude is the earthquake size on a log scale. We can also write the GR law as an energy-frequency relation. The conversion between the energy release and the moment magnitude is $M_w = (\frac{2}{3}) \log_{10}(E) - 3.2$ (so $S \propto E^{2/3}$; this gives rise to the energy-frequency relation, $\mathbb{P}(\text{Energy} > E) \propto E^{-B}$, where the exponent $B = \frac{2}{3}b$). For our analysis, we use a historical dataset from the US Geological Survey, which contains all 23,412 significant earthquakes with a magnitude of 5.5 or higher from 1965 to 2016.

In figure 2a we show the sub-sampled BMs of the earthquake energy release together with the MPMR (the most probable maximum energy, obtained from mode estimate) and EMR (the expected maximum energy, estimated as the sample mean) at various sample sizes n . The log-log plots of MPMR versus the sample size show a scaling relation: $E_{\text{MPMR}}(n) \approx 2.15 \times 10^{13} n^\eta$

Joules, where the SE, $\eta \approx 1.257$. From this scaling relation, we can expect the energy of the maximum earthquake in one year (we use $n = 450$, which is the average number of earthquakes in one year in the data set) $\approx 4.67 \times 10^{16}$ Joules (the magnitude $M_w \approx 7.91$), the energy of the maximum earthquake in 10 years $\approx 8.44 \times 10^{17}$ Joules ($M_w \approx 8.75$), and the energy of the maximum earthquake in 100 years $\approx 1.53 \times 10^{19}$ ($M_w \approx 9.58$), which is close to the magnitude of the great 1960 Chilean earthquake. The SE of $\eta = 1.257$ gives rise to the tail index TI, $B = 0.79$ and $b = 1.19$. This B -value is quite close to the B -value (≈ 0.7) obtained from a quasi-static model of earthquakes in an earthquake zone with a pre-existing fault [23]. The SE obtained from the EMR is slightly smaller with $\eta \approx 1.15$ due to higher estimates obtained for the EMR for small n . The MPMR and EMR converge as the sample size increases.

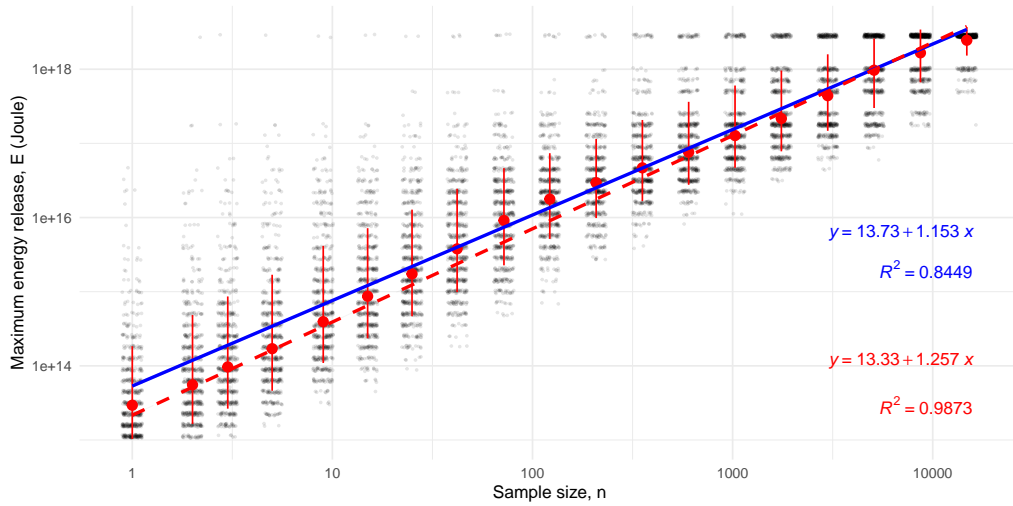
In figure 2b we show the time series of MPMR, EMR, and TI estimates, using aggregated observations within each year. Since the counts of observations are changing, we set the sample size as $1 - \frac{1}{e}$ of the counts in each aggregation. The maximum energy estimates based on MPMR and EMR are very close for these sample sizes. Note that the estimated TI (B -value) based on earthquake statistics within a year varies from year to year in the range of 0.56 to 0.93 and is shown negatively correlated with the MPMR.

4.2. Tsunami

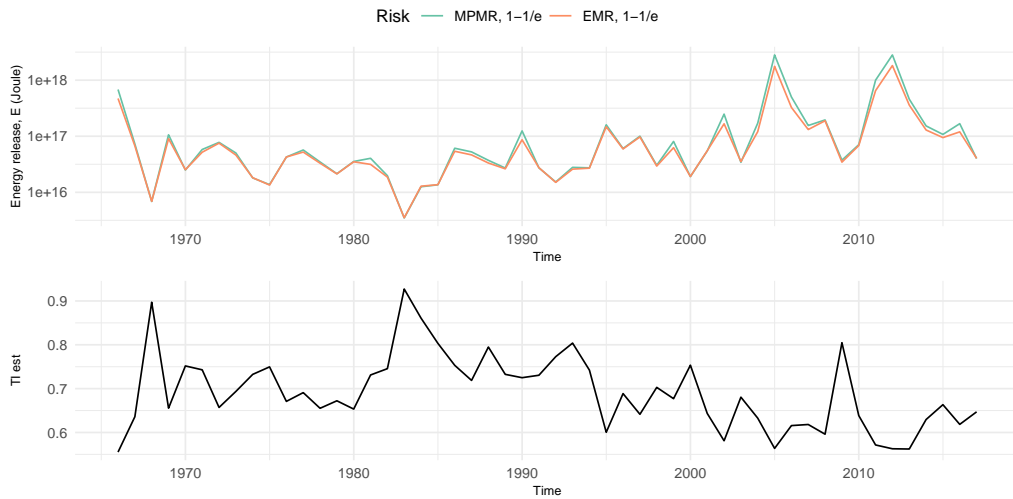
In the second example, we turn to Tsunami statistics. We use the data from NGDC/WDS Global Historical Tsunami Database [45].

In figure 3a we show the sub-sampled BMs together with the MPMR and EMR estimates of the maximum water height in tsunami events. The power-law scaling works well for the dependence of MPMR and EMR on the number of tsunamis in the sample; the dependence is estimated as $n^{0.86}$. This corresponds to the TI, $\xi \approx 1.16$ for the maximum water height distribution. The statistics of tsunami sizes should be related to the corresponding earthquake statistics. Our empirical analysis suggests $b \approx 1.19$, which is close to the tail index for tsunami water height $\xi \approx 1.16$. This suggests the relation between the maximum water height H and the earthquake magnitude: $M_w \approx \log(H) + \text{const}$, consistent with the empirical analysis of Abe [46].

In figure 3b we show the time series of MPMR, EMR, and TI estimates,



(a) Maximum energy release among n earthquake occurrences. Red bars cover mean \pm sd. Red dots mark mode estimates. The blue solid line fits all data and the red dashed line fits mode estimates.



(b) Time series of earthquake MPMR, EMR, and TI, using observations within each year.

Figure 2

using aggregated observations every ten years. We set the sample size as $1 - \frac{1}{e}$ of the number in each aggregation. The MPMR and EMR are very close in most cases but there are discrepancies at some time intervals due to very small raw sample sizes.

4.3. Rainfall

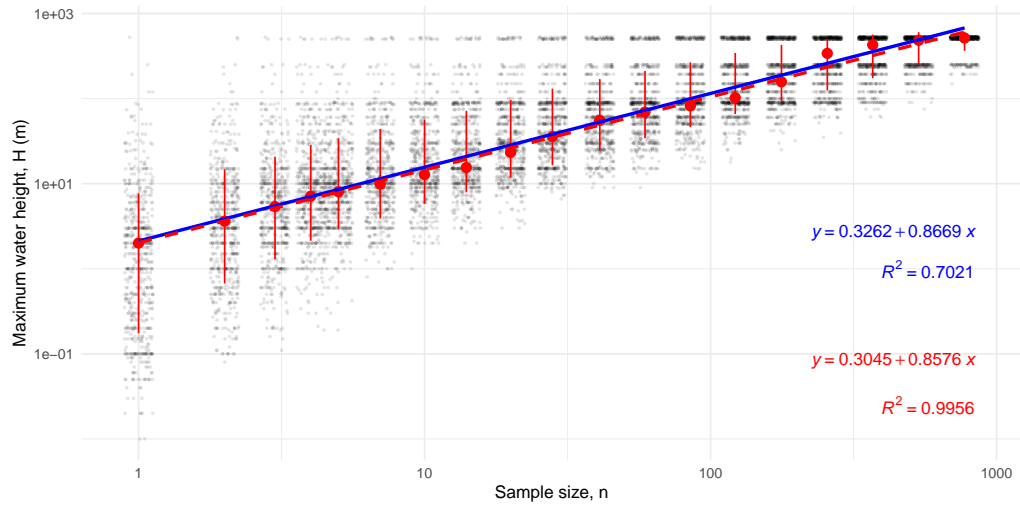
In the third example, we investigate the maximum monthly accumulated rainfall (monthly total precipitation) in monthly rainfall samples of various sizes. We use the data from the University of Delaware [47] which contains global monthly rainfall data from 1900 to 2008 (1308 months) at 85,794 locations. We remove the observations with 0 monthly total precipitation to focus on flood instead of drought hazards.

In figure 4a we show the sub-sampled BMs together with the MPMR and EMR estimates of maximum monthly total precipitation for a different number of months in the sample (sample size). To avoid the spatial-temporal proximal dependence that might deteriorate the i.i.d. assumption, we set the upper bound for the sample size as $n = 10,000$, which makes our samples sparse in space and time. From the figure, the maximum precipitation scales with n , the sample size, approximately $n^{0.35}$. This gives rise to the TI estimate of approximately 2.88.

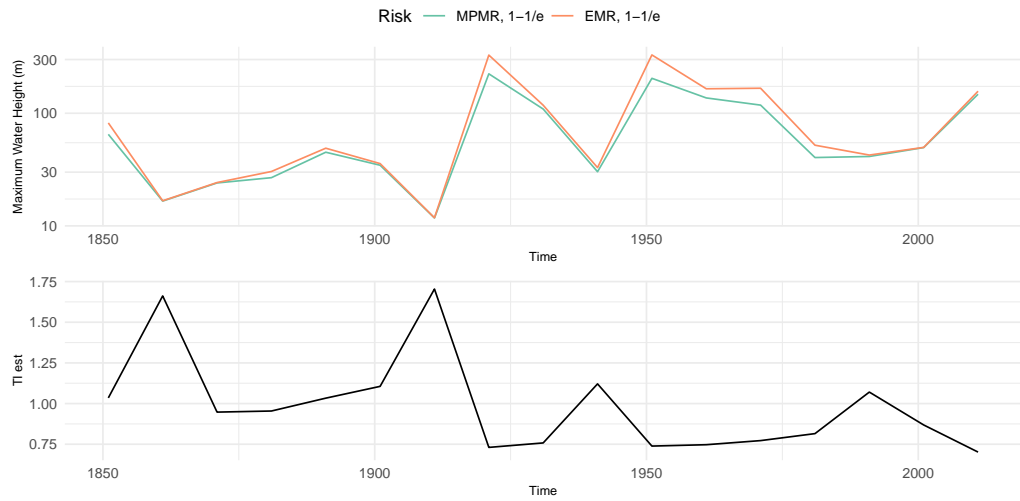
In figure 4b we show the time series of MPMR, EMR, and TI estimates, using aggregated observations within each year. In each aggregation, we have $12 \times 85,794 = 1,029,528$ observations, on which we sub-sample sparsely for either $n = 12$ or $n = 120$. The MPMR and EMR are close and the values are quite stable for more than 100 years. The TI shows some cyclical fluctuation, perhaps reflecting a certain time-series correlation. This remains to be explored in future research.

5. Stylized facts of MPMR/EMR on financial market risk

In this section, we focus again on financial risks and apply the proposed MPMR and EMR measures for estimating market risks. We use various market indices and bitcoin price series for our analysis; these include SP500 (from 1970-01-02 to 2022-07-29), HSI (from 1969-11-24 to 2022-06-30), NKY (from 1970-01-05 to 2022-06-30), and BTC (from 2017-09-02 to 2022-08-03). We consider the percentage log loss, $\text{loss} = \max(-\log_{\text{return}}, 0)$ (the loss is

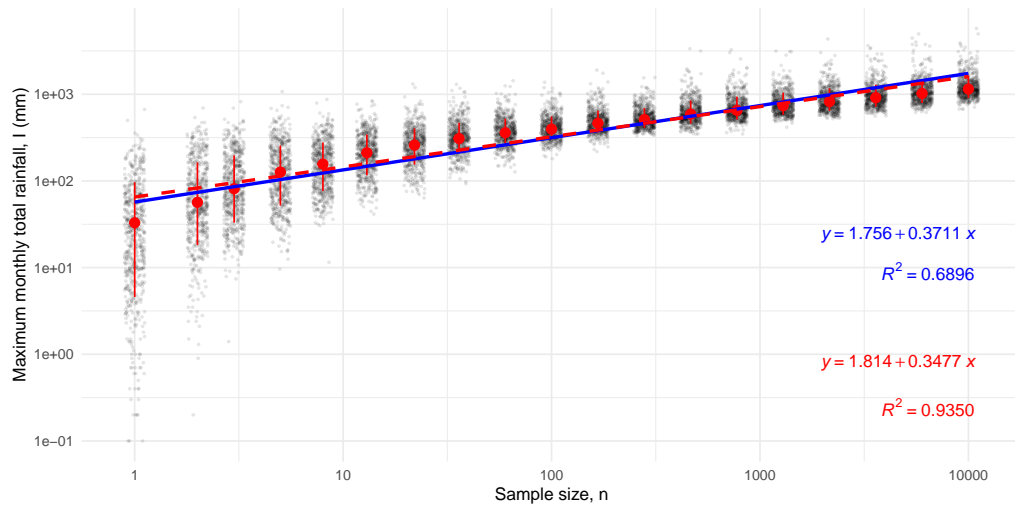


(a) Maximum water height among n tsunami occurrences. Red bars cover mean \pm sd. Red dots mark mode estimates. The blue solid line fits all data and the red dashed line fits mode estimates.

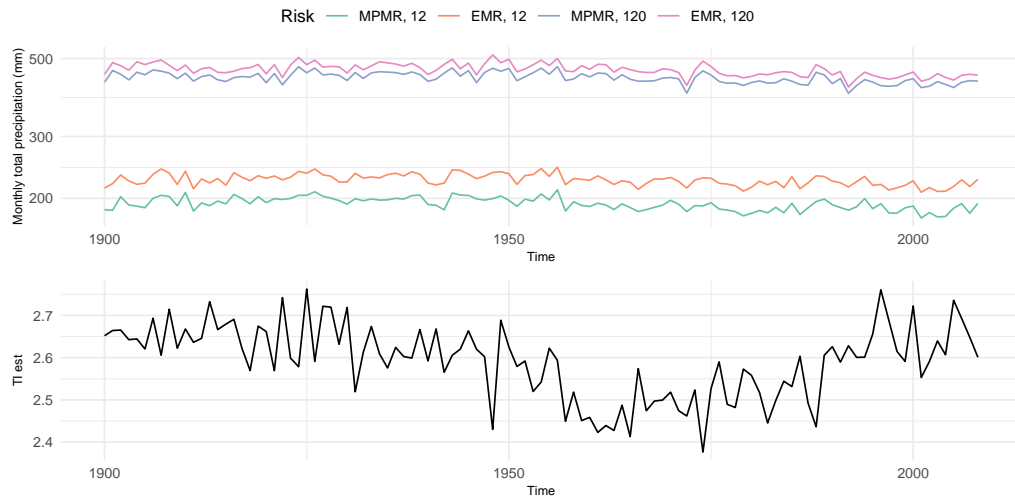


(b) Time series of tsunami MPMR, EMR, and TI, using observations every ten years.

Figure 3



(a) Maximum monthly accumulated rainfall (monthly total precipitation) among n months. Red bars cover mean \pm sd. Red dots mark mode estimates. The blue solid line fits all data and the red dashed line fits mode estimates.



(b) Time series of rainfall MPMR, EMR, and TI, using observations within each year.

Figure 4

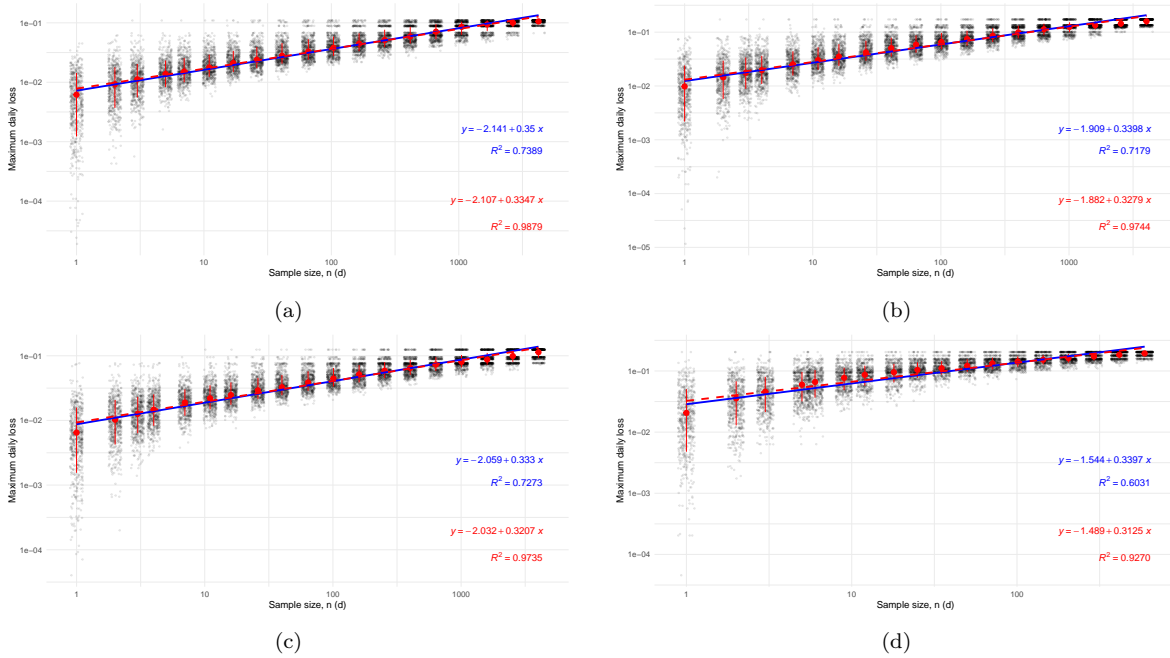


Figure 5: Maximum daily loss among n days, for (a) SP500, (b) HSI, (c) NKY, and (d) BTC. Red bars cover mean \pm sd. Red dots mark mode estimates. The blue solid line fits all data and the red dashed line fits mode estimates.

set to 0 for positive returns). To focus on the tail-risk behavior, we remove zero loss from the raw samples.

In figure 5 we show the sub-sampled BMs together with the MPMR and EMR estimates of the maximum daily loss for a different number of days in the sample (sample size). From the figure, we can see that the maximum loss scale with n , the sample size approximately as n^η . The scaling exponent η , estimated using either MPMR or EMR, is close to 0.33 for all the indices and BTC we consider. This gives rise to the TI estimate of approximately 3, strongly supporting the validity of the cubic law. The scaling relation can also be used to estimate the risk in a longer time frame than the time frame of the available data. For the SP500 index, the maximum daily loss is about 1.69% on average when $T = 10$ days, about 4.97% when the time frame is 1 year (corresponding to $T = 252$ trading days in a year), and about 10.74% when the time frame is 10 years. The scale invariance gives a reasonable estimate of about 23.21% when extrapolating to the time frame of 100 years.

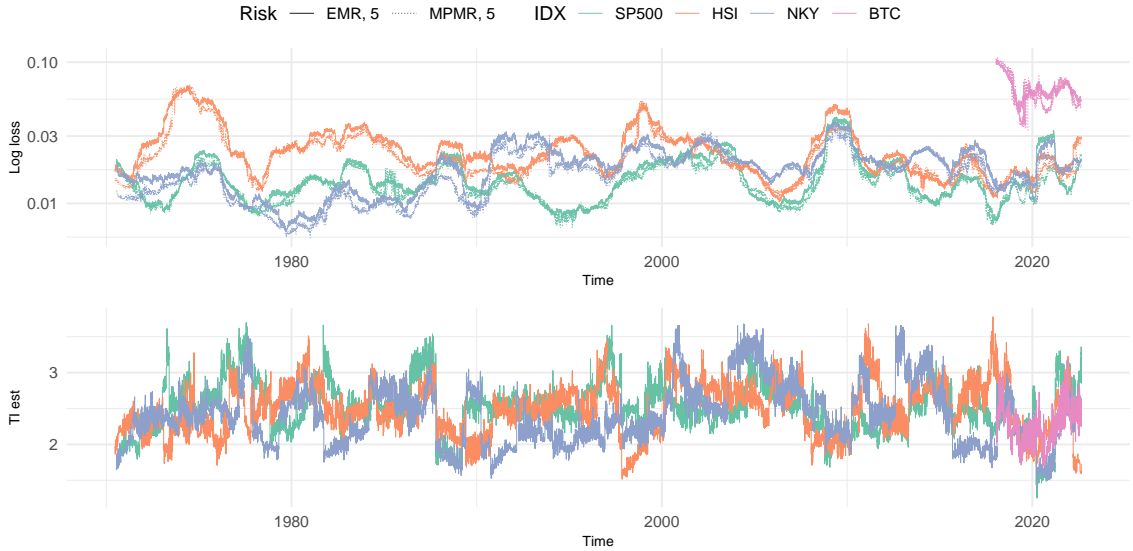


Figure 6: Time series of financial loss $MPMR_{5d}$, EMR_{5d} , and TI, using rolling 365d window.

In figure 6 we show the time series of MPMR, EMR, and TI estimates, using lagged rolling 365-day windows. Inside each window, we sub-sample with $n = 5$. The values of MPMR and EMR are very close, even for a small sample size of 5. The time series also show that the risk metrics of different assets rise together (indicating increasing correlations and worse diversification) in a stressed market. The TI shows strong oscillation in these 365-day rolling window estimates. Its dependence on the market condition is worth further investigation.

6. Conclusion

In this paper, we propose tail risk measures based on the maximum value of risk for a risk event within a time frame. We show the analytical forms of MPMR and EMR for several well-known underlying distributions. For the case of power-law tail distribution, the risk measure is shown to scale with the sample size with the scaling exponent η equal to the reciprocal of the tail index ξ : $\eta = 1/\xi$. By estimating η we can construct an estimator for

ξ . We have shown that such an estimator provides low-bias and consistent estimates (particularly for higher values of TIs, which are difficult to estimate directly but are widely seen in practice). We have shown robust sample-size scaling of the risk measures obtained from a wide range of data sources: from earthquakes, tsunamis, and rainfall, to financial market risks. This scale invariance helps relate the risks in different time frames and allows for using extrapolation to estimate the risk in a long time frame. Our analysis of the financial market risk using MPMR and EMR further validates the cubic law for the tail distribution of market risk; in particular, we have shown that the cubic law also applies to the cryptocurrency market. The analysis of the earthquake, tsunami, and rainfall data gives rise to a more intuitive measure of risks associated with such natural hazards in various time frames. These analyses also help to confirm some of the earlier theoretical and empirical results. The analysis of rainfall data gives stable estimates of MPMR and EMR spanning more than 100 years. Such assessments are important for managing long-term climate risks associated with extreme rainfall.

Acknowledgment

We thank Ms. Anzhi Liao for her help in conducting some simulations. This research is partly supported by a Ministry of Education academic research grant on Outbreak Resilience, Forecasting, and Early Warning.

References

- [1] X. D. He, S. Kou, X. Peng, Risk measures: robustness, elicibility, and backtesting, *Annual Review of Statistics and Its Application* 9 (2022) 141–166.
- [2] A. Adam, M. Houkari, J.-P. Laurent, Spectral risk measures and portfolio selection, *Journal of Banking & Finance* 32 (2008) 1870–1882. doi:[10.1016/j.jbankfin.2007.12.032](https://doi.org/10.1016/j.jbankfin.2007.12.032).
- [3] J. C. Hull, *Risk Management and Financial Institutions*, John Wiley & Sons, 2015.
- [4] A. C. Davison, R. Huser, Statistics of extremes, *Annual Review of Statistics and its Application* 2 (2015) 203–235.

- [5] M. I. Gomes, A. Guillo, Extreme Value Theory and Statistics of Univariate Extremes: A Review, *International Statistical Review / Revue Internationale de Statistique* 83 (2015) 263–292. Publisher: [Wiley, International Statistical Institute (ISI)].
- [6] N. Nolde, C. Zhou, Extreme Value Analysis for Financial Risk Management, *Annual Review of Statistics and Its Application* 8 (2021) 217–240. doi:[10.1146/annurev-statistics-042720-015705](https://doi.org/10.1146/annurev-statistics-042720-015705).
- [7] X. Gabaix, P. Gopikrishnan, V. Plerou, H. E. Stanley, A theory of power-law distributions in financial market fluctuations, *Nature* 423 (2003) 267–270. doi:[10.1038/nature01624](https://doi.org/10.1038/nature01624).
- [8] X. Gabaix, P. Gopikrishnan, V. Plerou, H. E. Stanley, Institutional Investors and Stock Market Volatility*, *The Quarterly Journal of Economics* 121 (2006) 461–504. doi:[10.1162/qjec.2006.121.2.461](https://doi.org/10.1162/qjec.2006.121.2.461).
- [9] H. E. Stanley, R. N. Mantegna, *An introduction to econophysics*, Cambridge University Press, Cambridge, 2000.
- [10] X. Gabaix, Power laws in economics: An introduction, *Journal of Economic Perspectives* 30 (2016) 185–206.
- [11] B. Kelly, H. Jiang, Tail risk and asset prices, *The Review of Financial Studies* 27 (2014) 2841–2871.
- [12] P. de Fontnouvelle, V. Dejesus-Rueff, E. S. Jordan, John S. & Rosengren, Capital and risk: New evidence on implications of large operational losses, *Journal of Money, Credit and Banking* 38 (2006) 1819–1846.
- [13] P. Burlando, R. Rosso, Scaling and multiscaling models of depth-duration-frequency curves for storm precipitation, *Journal of Hydrology* 187 (1996) 45–64.
- [14] H. Ghanmi, Z. Bargaoui, C. Mallet, Estimation of intensity-duration-frequency relationships according to the property of scale invariance and regionalization analysis in a mediterranean coastal area, *Journal of Hydrology* 541 (2016) 38–49.
- [15] P. Bak, *How nature works: the science of self-organized criticality*, Copernicus, 1999.

- [16] P. Bak, K. Chen, Self-organized criticality, *Scientific American* 264 (1991) 46–53.
- [17] J. P. Sethna, Power laws in physics, *Nature Reviews Physics* (2022) 1–3.
- [18] P. Bak, C. Tang, K. Wiesenfeld, Self-organized criticality: An explanation of the $1/f$ noise, *Physical review letters* 59 (1987) 381.
- [19] J. M. Carlson, J. Langer, B. E. Shaw, C. Tang, Intrinsic properties of a burridge-knopoff model of an earthquake fault, *Physical Review A* 44 (1991) 884.
- [20] K. Chen, P. Bak, S. P. Obukhov, Self-organized criticality in a crack-propagation model of earthquakes, *Physical Review A* 43 (1991) 625.
- [21] J. B. Rundle, D. L. Turcotte, W. Klein, *Geocomplexity and the Physics of Earthquakes*, the American Geophysical Union, 2000.
- [22] A. Sornette¹, D. Sornette, Self-organized criticality and earthquakes, *Europhysics Letters* 9 (1989) 197.
- [23] K. Chen, R. Bhagavatula, C. Jayaprakash, Earthquakes in quasistatic models of fractures in elastic media: formalism and numerical techniques, *Journal of Physics A: Mathematical and General* 30 (1997) 2297.
- [24] J.-P. Bouchaud, M. Potters, *Theory of Financial Risk and Derivative Pricing: From Statistical Physics to Risk Management*, Cambridge University Press, 2003.
- [25] I. F. D. Oliveira, R. H. C. Takahashi, An Enhancement of the Bisection Method Average Performance Preserving Minmax Optimality, *ACM Transactions on Mathematical Software* 47 (2021) 1–24. doi:[10.1145/3423597](https://doi.org/10.1145/3423597).
- [26] F. Johansson, Computing the lambert w function in arbitrary-precision complex interval arithmetic, *Numerical Algorithms* 83 (2020) 221–242.
- [27] B. I. Schneider, B. R. Miller, B. V. Saunders, Nist’s digital library of mathematical functions, *Physics today* 71 (2018).

- [28] J. C. Lee, J. Li, C. Musco, J. M. Phillips, W. M. Tai, Finding an Approximate Mode of a Kernel Density Estimate, in: P. Mutzel, R. Pagh, G. Herman (Eds.), 29th Annual European Symposium on Algorithms (ESA 2021), volume 204 of *Leibniz International Proceedings in Informatics (LIPIcs)*, Schloss Dagstuhl – Leibniz-Zentrum für Informatik, Dagstuhl, Germany, 2021, pp. 61:1–61:19. doi:[10.4230/LIPIcs.ESA.2021.61](https://doi.org/10.4230/LIPIcs.ESA.2021.61), ISSN: 1868-8969.
- [29] Y. Aliyari Ghassabeh, On the convergence of the mean shift algorithm in the one-dimensional space, *Pattern Recognition Letters* 34 (2013) 1423–1427. doi:[10.1016/j.patrec.2013.05.004](https://doi.org/10.1016/j.patrec.2013.05.004).
- [30] H. Dhaker, E. H. Deme, Y. Ciss, β -divergence loss for the kernel density estimation with bias reduced, *Statistical Theory and Related Fields* 5 (2021) 221–231.
- [31] D. N. Politis, J. P. Romano, M. Wolf, On the asymptotic theory of subsampling, *Statistica Sinica* (2001) 1105–1124.
- [32] C. M. Crainiceanu, A. Crainiceanu, The upstrap, *Biostatistics* 21 (2020) e164–e166. doi:[10.1093/biostatistics/kxy054](https://doi.org/10.1093/biostatistics/kxy054).
- [33] R. R. Wilcox, The bootstrap, in: *Fundamentals of modern statistical methods*, Springer, 2010, pp. 87–108.
- [34] R. Munasinghe, P. Kossinna, D. Jayasinghe, D. Wijeratne, Fast tail index estimation for power law distributions in r, *arXiv preprint arXiv:2006.10308* (2020).
- [35] I. Fedotenkov, A Review of More than One Hundred Pareto-Tail Index Estimators, *Statistica* 80 (2020) 245–299. doi:[10.6092/issn.1973-2201/9533](https://doi.org/10.6092/issn.1973-2201/9533), number: 3.
- [36] B. M. Hill, A simple general approach to inference about the tail of a distribution, *The annals of statistics* (1975) 1163–1174.
- [37] H. M. Zaher, A. A. El-Sheik, N. A. A. El-Magd, Estimation of pareto parameters using a fuzzy least-squares method and other known techniques with a comparison, *British Journal of Mathematics & Computer Science* 4 (2014) 2067.

- [38] J. Nair, A. Wierman, B. Zwart, The fundamentals of heavy-tails: Properties, emergence, and identification, in: Proceedings of the ACM SIGMETRICS/international conference on Measurement and modeling of computer systems, 2013, pp. 387–388.
- [39] S. H. Bhatti, S. Hussain, T. Ahmad, M. Aslam, M. Aftab, M. A. Raza, Efficient estimation of pareto model: Some modified percentile estimators, *PloS one* 13 (2018) e0196456.
- [40] M. E. Newman, Power laws, pareto distributions and zipf’s law, *Contemporary physics* 46 (2005) 323–351.
- [41] V. Brazauskas, R. Serfling, Robust and efficient estimation of the tail index of a single-parameter pareto distribution, *North American Actuarial Journal* 4 (2000) 12–27.
- [42] M. Rytgaard, Estimation in the pareto distribution, *ASTIN Bulletin: The Journal of the IAA* 20 (1990) 201–216.
- [43] S. Wager, Subsampling extremes: From block maxima to smooth tail estimation, *Journal of Multivariate Analysis* 130 (2014) 335–353. doi:[10.1016/j.jmva.2014.06.010](https://doi.org/10.1016/j.jmva.2014.06.010).
- [44] I. D. Haigh, T. Wahl, *Advances in extreme value analysis and application to natural hazards*, 2019.
- [45] N. P. Arcos, C. Slater, P. K. Dunbar, K. J. Stroker, R. Klucik, Past, present, and future: Interface for the ncei/wds global historical tsunami database, in: *AGU Fall Meeting Abstracts*, volume 2019, 2019, pp. NH43F–0992.
- [46] K. Abe, Size of great earthquakes of 1837–1974 inferred from tsunami data, *Journal of Geophysical Research: Solid Earth* 84 (1979) 1561.
- [47] K. Matsuura, C. J. Willmott, *Terrestrial precipitation: 1900–2017 gridded monthly time series*, Electronic. Department of Geography, University of Delaware, Newark, DE 19716 (2018).